



Efficient mass- and energy-preserving schemes for the coupled nonlinear Schrödinger–Boussinesq system

Jiaxiang Cai^{a,b,*}, Bin Yang^a, Chun Zhang^a

^a School of Mathematical Science, Huaiyin Normal University, Huaian Jiangsu 223300, China

^b Department of Mathematics, Purdue University, West Lafayette, IN 47907, USA

ARTICLE INFO

Article history:

Received 7 October 2018

Received in revised form 26 November 2018

Accepted 26 November 2018

Available online 3 December 2018

Keywords:

Schrödinger–Boussinesq equation

Hamiltonian system

Discrete gradient method

Fast Fourier transform

ABSTRACT

Efficient, mass- and energy-preserving schemes are developed for the multi-dimensional coupled nonlinear Schrödinger–Boussinesq system. In the scheme, the solution u^{n+1} is decoupling of v^{n+1} and ϕ^{n+1} . A fast solver is proposed to speed up the computation of the solutions v^{n+1} and ϕ^{n+1} . Numerical results show that our scheme gives better solution than the existing schemes, and also verify that it has the exact preservation of the discrete mass and energy.

© 2018 Elsevier Ltd. All rights reserved.

1. Introduction

In recent years, the Schrödinger-type equations, plasma model and fluid dynamics have attracted much attention [1–4]. The coupled nonlinear Schrödinger–Boussinesq (CNSB) system [5,6] is

$$\begin{cases} iu_t + \gamma \Delta u - \xi uv = 0, & i^2 = -1, \\ v_t - \Delta \phi = 0, \\ \phi_t - v + \alpha \Delta v - f(v) - \omega |u|^2 = 0, \end{cases} \quad (1)$$

where the complex function $u(x, t)$ and the real function $v(x, t)$, $x = (x_1, \dots, x_d)^\top \in \mathbb{R}^d$, $t \in (0, T]$, represent the electric field of Langmuir oscillations and the low-frequency density perturbation, respectively, the parameters $\gamma, \xi, \alpha > 0$ are real constants and $f(\cdot)$ is a sufficiently smooth real function with $f(0) = 0$. The system describes various physical processes in the field of laser and plasma, such as the interaction of long waves with short wave pockets in nonlinear dispersive media and diatomic lattice system [7], and the dynamics behavior of Langmuir soliton formation [8]. In practical computation, the CNSB system is usually

* Corresponding author at: School of Mathematical Science, Huaiyin Normal University, Huaian Jiangsu 223300, China.
E-mail addresses: cjx1981@hytc.edu.cn, thomasjeer@sohu.com (J. Cai).

truncated on a bounded Ω which is an interval in one dimension ($d = 1$), a rectangle in two dimensions ($d = 2$) or a box in three dimensions ($d = 3$). In this letter, we focus on developing efficient conservative schemes for the CNSB system with initial conditions $u_0(\mathbf{x}) = u(\mathbf{x}, 0)$, $v_0(\mathbf{x}) = v(\mathbf{x}, 0)$, $\phi_0(\mathbf{x}) = \phi(\mathbf{x}, 0)$, $\mathbf{x} \in \Omega$, and $(l_1, \dots, l_d)^\top$ -periodic boundary conditions. The periodic-initial value problem implies the total mass

$$I_1(t) := \int_{\Omega} |u(\mathbf{x}, t)|^2 d\mathbf{x} \equiv I_1(0) = \int_{\Omega} |u_0(\mathbf{x})|^2 d\mathbf{x} \quad (2)$$

and total energy

$$I_2(t) := \int_{\Omega} v^2 + |\nabla \phi|^2 + \frac{2\omega\gamma}{\xi} |\nabla u|^2 + \alpha |\nabla v|^2 + 2F(v) + 2\omega v |u|^2 d\mathbf{x} \equiv I_2(0), \quad (3)$$

where $F(v)$ is a primitive function of $f(v)$ and $|\nabla u|^2 = \sum_{j=1}^d |\partial_{x_j} u|^2$.

For the system in one dimension, there have been a few numerical studies, such as mass- and energy-preserving methods [9–11], multisymplecticity-preserving method [12] and orthogonal spline collocation methods [13]. These schemes exhibit excellent numerical performance, but it is difficult to extend them to the multi-dimensional system since their fully coupled and nonlinearly implicit features result in the low computational efficiency and amount of memory requirement as solving the obtained nonlinear system. Till now, few numerical methods can be available in the literature for the CNSB system in $d \geq 2$ dimensions except the non-energy-preserving method in [14].

Sometimes, conservation of both the mass and energy plays important role in the simulation of wave evolution. The main purpose of this study is to develop efficient, mass- and energy-preserving schemes for the CNSB system (1). To this end, firstly the system is cast into an infinite Hamiltonian form. Secondly, Fourier pseudospectral and coordinate increment discrete gradient (CIDG) is employed to develop conservative scheme in which the solution \mathbf{u}^{n+1} is decoupling of \mathbf{v}^{n+1} and Φ^{n+1} while the solutions \mathbf{v}^{n+1} and Φ^{n+1} are coupled. Thanks to the discrete fast Fourier transform (DFFT), a fast solver is proposed to speed up the numerical computation of \mathbf{v}^{n+1} and Φ^{n+1} . Finally, the composing technique [15,16] is employed to increase the order in time while preserving discrete mass and energy of the basic scheme.

2. Mass- and energy-preserving scheme

In this section, we only deal with the CNSB system in two dimensions, i.e., $d = 2$, $\mathbf{x} = (x, y)$ and $\Omega = [x_l, x_r] \times [y_l, y_r]$. The system in one dimension, three dimensions or higher dimensions can be solved analogously. For a positive integer N , let $t_n = n\tau$, $0 \leq n \leq N$, where the temporal increment $\tau = T/N$, and for the two positive integers J and K , let the space-step sizes be $h_x = (x_r - x_l)/J$ and $h_y = (y_r - y_l)/K$.

By setting the complex function $u(x, y, t) = p(x, y, t) + iq(x, y, t)$ where $p(x, y, t)$ and $q(x, y, t)$ are real functions, one can rewrite the system (1) as an infinite Hamiltonian form

$$\dot{w} = \mathcal{D} \frac{\delta \mathcal{H}}{\delta w}, \quad (4)$$

where $w = (p, q, v, \psi)^\top$, the dot denotes ∂_t , the functional $\mathcal{H} = I_2(t)$ and the skew-adjoint linear differential operator

$$\mathcal{D} = \begin{pmatrix} \xi \mathcal{P}/(4\omega) & 0 \\ 0 & -\mathcal{P}/2 \end{pmatrix}, \quad \mathcal{P} = \begin{pmatrix} 0 & 1 \\ -1 & 0 \end{pmatrix}. \quad (5)$$

The Hamiltonian system (4) holds symplecticity and energy, simultaneously. Sometimes, conservation of energy plays a more important role than the preservation of symplecticity, especially in the simulation of solitons. Recently, several energy- or integral-preserving methods have been proposed for ODEs and PDEs such as the discrete gradients and discrete variational derivative methods [17–20]. After suitable spatial

discretizations of the skew-adjoint operator and Hamiltonian in (4), one has the following finite dimensional Hamiltonian system

$$\dot{\mathbf{w}} = \overline{\mathcal{D}} \nabla_{\mathbf{w}} \overline{\mathcal{H}}, \quad (6)$$

where $\mathbf{w} = (\mathbf{p}^\top, \mathbf{q}^\top, \mathbf{v}^\top, \Phi^\top)^\top$, $\mathbf{p}, \mathbf{q}, \mathbf{v}, \Phi \in \mathbb{R}^{J \times K}$ with $\mathbf{p} = (p_{j,k})$, $\mathbf{q} = (q_{j,k})$, $\mathbf{v} = (v_{j,k})$ and $\Phi = (\phi_{j,k})$, $\nabla_{\mathbf{w}} \overline{\mathcal{H}} = \frac{\delta}{\delta \mathbf{w}} (\overline{\mathcal{H}} h_x h_y)$ and

$$\begin{aligned} \overline{\mathcal{D}} &= \begin{pmatrix} \xi \overline{\mathcal{P}} / (4\omega) & \mathbf{0} \\ \mathbf{0} & -\overline{\mathcal{P}} / 2 \end{pmatrix}, \quad \overline{\mathcal{P}} = \begin{pmatrix} \mathbf{0} & \text{id} \\ -\text{id} & \mathbf{0} \end{pmatrix}, \quad \text{id} \in \mathbb{R}^{J \times J} \\ \overline{\mathcal{H}} &= \sum_{j,k} (B_x \otimes \Phi)_{j,k}^2 (B_y \otimes \Phi)_{j,k}^2 + \frac{2\omega\gamma}{\xi} ((B_x \otimes \mathbf{p})_{j,k}^2 + (B_x \otimes \mathbf{q})_{j,k}^2 + (B_y \otimes \mathbf{p})_{j,k}^2 + (B_y \otimes \mathbf{q})_{j,k}^2) \\ &\quad + v_{j,k}^2 + \alpha((B_x \otimes \mathbf{v})_{j,k}^2 + (B_y \otimes \mathbf{v})_{j,k}^2) + 2F(v_{j,k}) + 2\omega v_{j,k} |u_{j,k}|^2. \end{aligned} \quad (7)$$

Here, B_x and B_y are any circulant skew-symmetric differential matrices. The system (6) possesses the Hamiltonian $\overline{\mathcal{H}}$ due to the skew-symmetric property of the matrix $\overline{\mathcal{D}}$, so that it is natural to integrate it in time with a conservative method. In general, the DG methods can be employed. Here the choice of CIDG method [16,21] reads the scheme $\delta_t \mathbf{w}^n = \overline{\mathcal{D}} \nabla_{\mathbf{w}} \overline{\mathcal{H}}(\mathbf{w}^{n+1}, \mathbf{w}^n)$, i.e.,

$$\begin{aligned} i\delta_t \mathbf{u}^n + \gamma \underline{\Delta} A_t \mathbf{u}^n &= \xi \mathbf{v}^n A_t \mathbf{u}^n, \quad \delta_t \mathbf{v}^n = \underline{\Delta} A_t \Phi^n, \\ \delta_t \Phi^n - A_t \mathbf{v}^n + \alpha \underline{\Delta} A_t \mathbf{v}^n &= \frac{F(\mathbf{v}^{n+1}) - F(\mathbf{v}^n)}{\mathbf{v}^{n+1} - \mathbf{v}^n} + \omega |\mathbf{u}^{n+1}|^2, \end{aligned} \quad (8)$$

where δ_t represents the Euler forward finite difference operator and $\underline{\Delta} = B_x^2 \otimes + B_y^2 \otimes$.

Theorem 2.1. *The scheme (8) is mass- and energy-preserving, which captures the discrete mass $\mathcal{I}_1^n = \|\mathbf{u}^n\|^2 = \dots = \mathcal{I}^0 = \|\mathbf{u}^0\|^2$ and the discrete energy $\mathcal{I}_2^n = \overline{\mathcal{H}}^n h_x h_y = \dots = \mathcal{I}_2^0 = \overline{\mathcal{H}}^0 h_x h_y$.*

Proof. Taking the discrete inner product of the first equation in (8) with $A_t \mathbf{u}^n$ gives the mass invariant, immediately. The application of the CIDG to (6) implies the energy invariant. This completes the proof. \square

Remark 2.1. The mass- and energy-preserving scheme (8) is of order 1 in time because CIDG is of order 1. One can propose a temporal second-order energy-preserving scheme by integrating (6) with the second-order averaged vector field method [22], however the obtained scheme is non-mass-preserving and fully coupled.

2.1. Temporal second-order scheme

The energy-preserving scheme (8) has spectral accuracy in space, while first-order accuracy in time. In practice, the temporal second-order scheme is desired. To end this, one can develop it by making use of the composing method [15,16].

Definition 2.1. Let $\Phi_\tau : \mathbf{y}^n \rightarrow \mathbf{y}^{n+1}$ be a basic one-step numerical method for the autonomous ODEs $\mathbf{y} = f(\mathbf{y})$, $\mathbf{y}(t_0) = \mathbf{y}_0$. The adjoint method $\tilde{\Phi}_\tau$ of the method Φ_τ is the inverse map of the original method with reversed time step $-\tau$, i.e., $\tilde{\Phi}_\tau = \Phi_{-\tau}^{-1}$.

Theorem 2.2 ([16]). *Let Φ_τ be a one-step method of order 1 and $\tilde{\Phi}_\tau$ be the adjoint of Φ_τ . Then $\Psi_\tau = \tilde{\Phi}_{\tau/2} \circ \Phi_{\tau/2}$ is a second-order symmetric method.*

Let $\bar{\nabla}^* \bar{\mathcal{H}}(\hat{u}, u) = \bar{\nabla} \bar{\mathcal{H}}(u, \hat{u})$ be a discretization of $\bar{\mathcal{H}}$. Clearly, $\bar{\nabla}^*$ is also a DG of $\bar{\mathcal{H}}$. An application of it to (6) gives a new scheme $\delta_t w^n = \bar{\mathcal{D}} \bar{\nabla} \bar{\mathcal{H}}(w^n, w^{n+1})$, i.e.,

$$\begin{aligned} i\delta_t u^n + \gamma \underline{\Delta} A_t u^n &= \xi v^{n+1} A_t u^n, \quad \delta_t v^n = \underline{\Delta} A_t \Phi^n, \\ \delta_t \Phi^n - A_t v^n + \alpha \underline{\Delta} A_t v^n &= \frac{F(v^{n+1}) - F(v^n)}{v^{n+1} - v^n} + \omega |u^n|^2. \end{aligned} \quad (9)$$

Clearly, it is mass- and energy-preserving, and u^{n+1} is decoupling of v^{n+1} and Φ^{n+1} . It follows from Definition 2.1 that (9) is adjoint to (8). Denote the schemes (8) and (9) by the maps: $\psi_\tau, \tilde{\psi}_\tau : (u^n, v^n, \Phi^n) \rightarrow (u^{n+1}, v^{n+1}, \Phi^{n+1})$, respectively. By Theorem 2.2, one immediately has a temporal second-order, mass- and energy-preserving scheme

$$\Psi_\tau = \tilde{\psi}_{\tau/2} \circ \psi_{\tau/2} : (u^n, v^n, \Phi^n) \rightarrow (u^{n+1}, v^{n+1}, \Phi^{n+1}). \quad (10)$$

3. A fast solver

Lemma 3.1 ([23]). Any circulant square matrix A can be diagonalized, i.e., $A = \mathcal{F}^{-1} \Lambda_A \mathcal{F}$, where \mathcal{F} is the matrix of discrete Fourier transform coefficients with entries given by $(\mathcal{F})_{r,s} = (e^{-i2\pi/N})^{rs}$, \mathcal{F}^{-1} is the matrix of inverse discrete Fourier transform with entries $(\mathcal{F}^{-1})_{r,s} = \frac{1}{N} (e^{i2\pi/N})^{rs}$, and Λ_A is a diagonal matrix with diagonal entries $\text{diag}(\Lambda_A) = \mathcal{F}a$ where a is the first column of A .

The lemma is helpful for improving the computational efficiency of the present schemes. For example, the scheme (8) can be reformed into the form

$$\begin{aligned} i\delta_t \tilde{u}^n + \gamma \underline{\Delta} A_t \tilde{u}^n &= \xi \widetilde{v^n A_t u^n}, \quad \delta_t \tilde{v}^n = \underline{\Delta} A_t \tilde{\Phi}^n, \\ \delta_t \tilde{\Phi}^n - A_t \tilde{v}^n + \alpha \underline{\Delta} A_t \tilde{v}^n &= \widetilde{F(v^{n+1}, v^n)} + \omega |\widetilde{u^{n+1}}|^2, \end{aligned} \quad (11)$$

where $\tilde{u}^n = \mathcal{F}_x \otimes \mathcal{F}_y \otimes u^n$, $\underline{\Delta} = \Lambda_{B_x}^2 \otimes \Lambda_{B_y}^2$ and $\widetilde{F(v^{n+1}, v^n)} = \mathcal{F}_x \otimes \mathcal{F}_y \otimes \left(\frac{F(v^{n+1}) - F(v^n)}{v^{n+1} - v^n} \right)$. It follows from (11) that

$$\begin{aligned} i\delta_t \tilde{u}_{j,k}^n + \gamma \underline{\Delta}_{j,k} A_t \tilde{u}_{j,k}^n &= \xi (\widetilde{v^n A_t u^n})_{j,k}, \quad \delta_t \tilde{v}_{j,k}^n = \underline{\Delta}_{j,k} A_t \tilde{\Phi}_{j,k}^n, \\ \delta_t \tilde{\Phi}_{j,k}^n - A_t \tilde{v}_{j,k}^n + \alpha \underline{\Delta}_{j,k} A_t \tilde{v}_{j,k}^n &= \widetilde{F_{j,k}(v^{n+1}, v^n)} + \omega (\widetilde{|u^{n+1}|^2})_{j,k}, \end{aligned} \quad (12)$$

where $\underline{\Delta}_{j,k} = (\Lambda_{B_x})_{j,j}^2 + (\Lambda_{B_y})_{k,k}^2$. Eq. (12) is equivalent to the form

$$\begin{aligned} \tilde{u}_{j,k}^{n+1} &= ((2i - \tau\gamma \Lambda_{j,k}) + \tau\xi (\widetilde{v^n A_t u^n})_{j,k}) / (2i + \tau\gamma \Lambda_{j,k}), \\ \tilde{v}_{j,k}^{n+1} &= ((1 + A_{j,k})\tilde{v}_{j,k}^n + \tau\Lambda_{j,k}\tilde{\Phi}_{j,k}^n + \frac{\tau^2}{2}\Lambda_{j,k}\widetilde{NT}_{j,k}) / (1 - A_{j,k}), \\ \tilde{\Phi}_{j,k}^{n+1} &= (\tau(1 - \alpha\Lambda_{j,k})\tilde{v}_{j,k}^n + (1 + A_{j,k})\tilde{\Phi}_{j,k}^n + \tau\widetilde{NT}_{j,k}) / (1 - A_{j,k}), \end{aligned} \quad (13)$$

where $A_{j,k} = \frac{\tau^2}{4}(\Lambda_{j,k} - \alpha\Lambda_{j,k}^2)$ and $\widetilde{NT}_{j,k} = \widetilde{F_{j,k}(v^{n+1}, v^n)} + \omega (\widetilde{|u^{n+1}|^2})_{j,k}$, which can be solved efficiently by the fixed-point iteration method.

4. Numerical results

In this section, we report some numerical results to exhibit the performance of our second-order scheme. We mainly focus on the accuracy of the solution and the preservation of the discrete mass and energy. The accuracy of the solution at n th time level is scaled by the maximal error norm $L_\infty =$

Table 1The maximal errors in solution: $h_x = 1/4$, $T = 1$.

Method	$\tau = 1/16$	$\tau = 1/32$	$\tau = 1/64$
Present	3.8347e-3	9.5681e-4	2.3908e-4
TSFP [10] ($\beta = 1/2$)	2.6350e-2	6.6101e-3	1.6573e-3
Scheme I [13]	1.0656e-2	4.4113e-3	3.1175e-3
TS-EWI-FP [14]	6.6150e-3	1.6429e-3	4.0963e-4

Table 2The maximal errors in solution: $h_x = 1/4$, $T = 1$.

Method	$\tau = 1/16$	$\tau = 1/32$	$\tau = 1/64$
Present	2.984e-5	7.461e-6	1.865e-6
TSFP [10] ($\beta = 1/2$)	1.044e-4	2.639e-5	6.635e-6
Scheme I [13]	6.838e-5	3.825e-5	3.246e-5
TS-EWI-FP [14]	9.922e-5	2.497e-5	6.268e-6

$L_\infty^u + L_\infty^v$ and the average error norm $L_2 = L_2^u + L_2^v$ where $L_\infty^g = \max_{j,k} |g(x_j, y_k, t_n) - g_{j,k}^n|$ and $L_2^g = (h_x h_y \sum_{j,k} |g(x_j, y_k, t_n) - g_{j,k}^n|^2)^{1/2}$. The preservation of the mass and energy is monitored by $|\mathcal{I}_1^n - \mathcal{I}_1^0|$ and $|\mathcal{I}_2^n - \mathcal{I}_2^0|$, respectively. In the following simulations, we use the Fourier pseudo-spectral discretization in space [24].

One-dimensional CNSB system: For the case $f(v) = \theta v^2$, two types of analytical solution have been given in Refs. [8,25], i.e.,

(i) As $\gamma \xi d_1 = 2b_1(3\gamma\theta - \alpha\xi)$, $3\alpha\xi \neq \gamma\theta$ and $4\alpha b_1 \neq \gamma d_1$, $u(x, t) = \pm \frac{6b_1}{\xi} \sqrt{\frac{\gamma\theta - \alpha\xi}{\gamma\omega}} \text{sech}(\mu\zeta) \tanh(\mu\zeta) e^{i(\frac{\gamma}{2\gamma}x + \delta t)}$, $v(x, t) = -\frac{6b_1}{\xi} \text{sech}^2(\mu\zeta)$, $\phi(x, t) = \frac{12Sb_1}{\mu\xi} (\frac{x_r - x}{x_r - x_l} - \frac{1}{1+e^{2\mu\zeta}})$, $x \in [x_l, x_r]$, $t \geq 0$.

(ii) As $3\alpha\xi \neq \gamma\theta$ and $4\alpha b_1 \neq \gamma d_1$, $u(x, t) = \sqrt{\frac{6\alpha b_1}{\gamma^2 \theta \omega}} (\gamma d_1 - 4\alpha b_1) \text{sech}(\mu\zeta) e^{i(\frac{\gamma}{2\gamma}x + \delta t)}$, $v(x, t) = -\frac{6b_1}{\xi} \text{sech}^2(\mu\zeta)$, $\phi(x, t) = \frac{4Sb_1}{\mu\xi} (\frac{x_r - x}{x_r - x_l} - \frac{1}{1+e^{2\mu\zeta}})$, $x \in [x_l, x_r]$, $t \geq 0$. Here $b_1 = \delta + \frac{M^2}{4\gamma}$, $d_1 = 1 - M^2$, $\mu = \sqrt{b_1/\gamma}$, $\zeta = x - Mt$ and M, δ are free parameters.

Firstly, we choose $\gamma = 1$, $\xi = 1$, $\alpha = 2/3$, $\theta = 1/9$, $\omega = -1/2$, $M = \sqrt{22/15}$, $\delta = 1/3$, $\Omega = [-64, 64]$ and $T = 1$. Table 1 shows the L_∞ -error norms of our second-order scheme and the second-order schemes in the literature. Obviously, our scheme provides more accurate solution than the others.

Secondly, we solve the problem with $\gamma = 1$, $\xi = 1$, $\alpha = 1/2$, $\theta = 3/2$, $\omega = 1/12$, $M = \sqrt{1/3}$, $\delta = 1/5$, $\Omega = [-64, 64]$ and $T = 1$. Again, the solution of our scheme is the best (see Table 2). To show the long-term performance of our second-order scheme, the simulation is done up to $T = 10$ with $\tau = 1/64$ and $h_x = 1/4$. The results displayed in Fig. 1 show that our scheme exhibits satisfactory solution and preserves the two invariants exactly.

Two-dimensional CNSB system: Consider the system in two dimensions with $f(v) = \sin v$, parameters $\gamma = \alpha = 1$, $\xi = \omega = 1/10$ and the initial data $u_0(x, y) = \frac{2}{e^{x^2+2y^2} + e^{-(x^2+2y^2)}} e^{5i/\cosh(\sqrt{4x^2+y^2})}$, $v_0(x, y) = e^{-(x^2+y^2)}$, $\phi_0(x, y) = \frac{1}{2}e^{-(x^2+y^2)}$, $\Omega = (-40, 40) \times (-20, 20)$. The simulation is carried out with $\tau = 0.01$ and $h_x = h_y = 1/32$.

Fig. 2 displays the surface plots of $|u|$, v and ϕ at different times. The left plots show the initial hump collapses gradually as time evolves and two humps generate finally. The middle plots for the surface v show that a hole forms inside the hump and a spike appears under the horizontal plane gradually as the initial hump collapses. At time $t = 1$, one also see a solitary wave appears on the horizontal plane. The right plots display that the initial hump of ϕ also collapses and a solitary wave generates as time evolves, but no hole and spike generate. The changes in the mass and energy shown in the right graph of Fig. 1 verify our scheme conserves the invariants exactly.

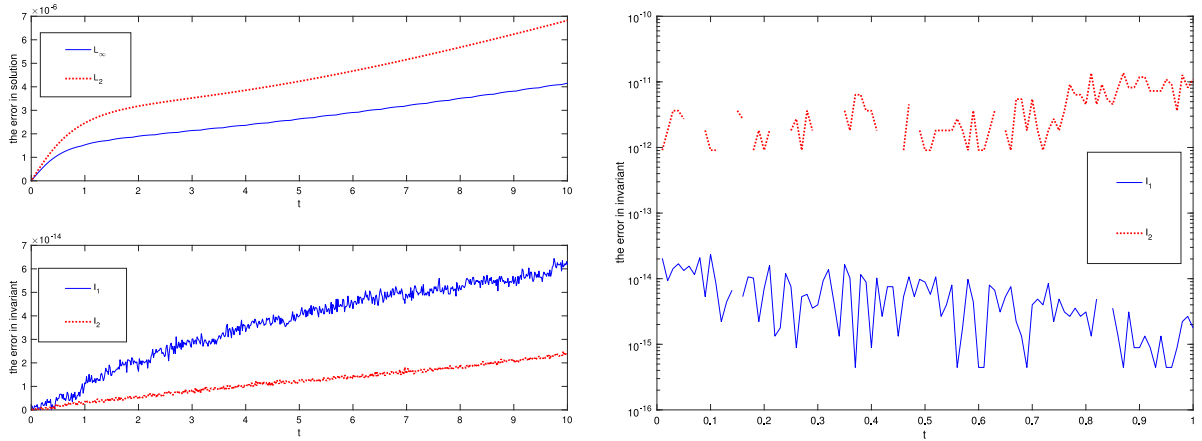


Fig. 1. Left: 1D problem; Right: 2D problem, the changes in invariants.

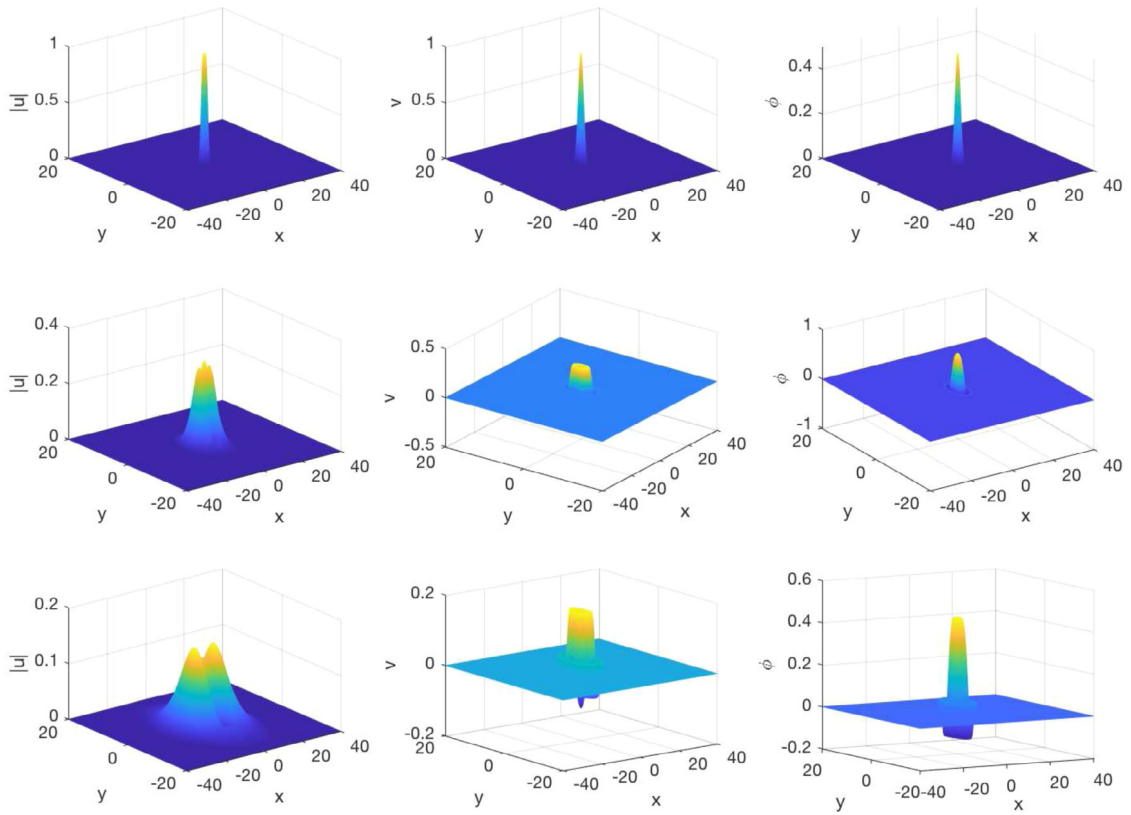


Fig. 2. Surface plots of $|u|$, v and ϕ at $t = 0$ (top), 0.5 (middle) and 1 (bottom), respectively.

5. Conclusion

Recently, much attention has been paid on the numerical studies for the CNSB system. Conservative methods are very popular for simulating the system because of their excellent long-term numerical performance. However, the existing conservative methods for the one-dimensional system are difficult to be extended to the multi-dimensional system due to the low computational efficiency of the obtained schemes. In this letter, we develop a second-order, mass- and energy-preserving, efficient scheme for the multi-dimensional

CNSB system, in which u^{n+1} is independent of v^{n+1} and Φ^{n+1} . Although v^{n+1} and Φ^{n+1} are coupled, a fast solver is proposed to speed up the numerical computation. Numerical results show that our scheme not only simulates the problem well, but also exhibits better performance than the existing schemes.

Acknowledgments

The work was supported by Natural Science Foundation of Jiangsu Province of China (BK20181482) and Jiangsu Overseas Visiting Scholar Program for University Prominent Young & Middle-aged Teachers and Presidents.

References

- [1] A. Taleei, M. Dehghan, Time-splitting pseudo-spectral domain method for the soliton solutions of the one- and multi-dimensional nonlinear Schrödinger equations, *Comput. Phys. Comm.* 185 (2014) 1515–1528.
- [2] M. Dehghan, Finite difference procedures for solving a problem arising in modeling and design of certain optoelectronic devices, *Math. Comput. Simulation* 71 (2006) 16–30.
- [3] M. Dehghan, A. Nikpour, The solitary wave solution of coupled Klein-Gordon-Zakharov equations via two different numerical methods, *Comput. Phys. Comm.* 184 (2013) 2145–2158.
- [4] M. Dehghan, R. Salehi, A mesh less based numerical technique for traveling solitary wave solution of Boussinesq equation, *Appl. Math. Model.* 36 (2012) 1939–1956.
- [5] V.G. Makhankov, On stationary solutions of the Schrödinger equation with a self-consistent potential satisfying Boussinesq's equation, *Phys. Lett. A* 50 (1974) 42–44.
- [6] V.E. Zakharov, Collapse of Langmuir waves, *Sov. Phys. JETP* 35 (1972) 908–914.
- [7] N. Yajima, J. Satsuma, Soliton solutions in a diatomic lattice system, *Progr. Theoret. Phys.* 62 (1979) 370–378.
- [8] N.N. Rao, Coupled scalar field equations for nonlinear wave modulations in dispersive media, *Pramana J. Phys.* 46 (1991) 161–202.
- [9] J.D. Zheng, M.M. Xiang, The finite element analysis for the equation system coupling the complex Schrödinger and real Boussinesq fields, *Math. Numer. Sin.* 2 (1984) 344–355, (in Chinese).
- [10] D.M. Bai, J.L. Wang, The time-splitting fourier spectral method for the coupled Schrödinger-Boussinesq equations, *Commun. Nonlinear Sci. Numer. Simul.* 17 (2012) 1201–1210.
- [11] F. Liao, L.M. Zhang, Conservative compact finite difference scheme for the coupled Schrödinger-Boussinesq equation, *Numer. Methods Partial Differential Equations* 32 (2016) 1667–1688.
- [12] L.Y. Huang, Y.D. Jiao, D.M. Liang, Multi-symplectic scheme for the coupled Schrödinger-Boussinesq equations, *Chin. Phys. B* 7 (2013) 1–5.
- [13] F. Liao, L.M. Zhang, S.S. Wang, Numerical analysis of cubic orthogonal spline collocation methods for the coupled Schrödinger-Boussinesq equations, *Appl. Numer. Math.* 119 (2017) 194–212.
- [14] F. Liao, L.M. Zhang, S.S. Wang, Time-splitting combining with exponential wave integrator Fourier pseudospectral method for Schrödinger-Boussinesq system, *Commun. Nonlinear Sci. Numer. Simul.* 55 (2018) 93–104.
- [15] H. Yoshida, Construction of higher order symplectic integrators, *Phys. Lett. A* 150 (1990) 262–268.
- [16] E. Hairer, C. Lubich, G. Wanner, *Geometric Numerical Integration: Structure-Preserving Algorithms for Ordinary Differential Equations*, Springer-Verlag, Berlin, 2006.
- [17] Y. Miyatake, T. Matsuo, A general framework for finding energy dissipative/conservative H^1 -Galerkin schemes and their underlying H^1 -weak forms for nonlinear evolution equations, *BIT* 54 (2014) 1119–1154.
- [18] J.X. Cai, J.L. Hong, Y.S. Wang, Y.Z. Gong, Two energy-conserved splitting methods for three-dimensional time-domain Maxwell's equations and the convergence analysis, *SIAM J. Numer. Anal.* 53 (2015) 1918–1940.
- [19] M. Dahlby, B. Owren, A general framework for deriving integral preserving numerical methods for PDEs, *SIAM J. Sci. Comput.* 33 (2011) 2318–2340.
- [20] J. Cai, Y. Wang, C. Jiang, Local structure-preserving algorithms for general multi-symplectic Hamiltonian PDEs, *Comput. Phys. Comm.* 235 (2019) 210–220.
- [21] T. Itoh, K. Abe, Hamiltonian-conserving discrete canonical equations based on variational difference quotients, *J. Comput. Phys.* 76 (1998) 85–102.
- [22] G.R.W. Quispel, D.I. McLaren, A new class of energy-preserving numerical integration methods, *J. Phys. A* 41 (2008) 1–7, 045206.
- [23] R.M. Gray, Toeplitz and circulant matrices: A review, 2006.
- [24] J. Cai, C. Bai, H. Zhang, Decoupled local/global energy-preserving schemes for the N -coupled nonlinear Schrödinger equations, *J. Comput. Phys.* 374 (2018) 281–299.
- [25] Y.R. Xia, L.Z. Bin, Exact explicit solutions of the nonlinear equation coupled to the Boussinesq equation, *Acta Math. Sci.* 23B (2003) 453–460.